



Since January 2020 Elsevier has created a COVID-19 resource centre with free information in English and Mandarin on the novel coronavirus COVID-19. The COVID-19 resource centre is hosted on Elsevier Connect, the company's public news and information website.

Elsevier hereby grants permission to make all its COVID-19-related research that is available on the COVID-19 resource centre - including this research content - immediately available in PubMed Central and other publicly funded repositories, such as the WHO COVID database with rights for unrestricted research re-use and analyses in any form or by any means with acknowledgement of the original source. These permissions are granted for free by Elsevier for as long as the COVID-19 resource centre remains active.



Nontoxic-dose deoxynivalenol aggravates lipopolysaccharides-induced inflammation and tight junction disorder in IPEC-J2 cells through activation of NF- κ B and LC3B

Lei Ge^{a,b,c}, Ziman Lin^{a,b,c}, Guannan Le^{a,b,c}, Lili Hou^{a,b,c}, Xinru Mao^{a,b,c}, Shuiping Liu^{a,b,c}, Dandan Liu^{a,b,c}, Fang Gan^{a,b,c}, Kehe Huang^{a,b,c,*}

^a College of Veterinary Medicine, Nanjing Agricultural University, Nanjing, 210095, Jiangsu Province, China

^b Institute of Nutritional and Metabolic Disorders in Domestic Animals and Fowls, Nanjing Agricultural University, Nanjing, 210095, Jiangsu Province, China

^c MOE Joint International Research Laboratory of Animal Health and Food Safety, College of Veterinary Medicine, Nanjing Agricultural University, Nanjing, 210095, Jiangsu Province, China

ARTICLE INFO

Keywords:

Deoxynivalenol
LPS
Inflammation
Tight junction
NF- κ B signaling pathway
LC3B

ABSTRACT

Lipopolysaccharide (LPS) is the key factor in various intestinal inflammation which could disrupt the epithelial barrier function. Deoxynivalenol (DON), a well-known mycotoxin, can induce intestinal injury. However, the combined enterotoxicity of LPS and DON has rarely been studied. In this study, IPEC-J2 cell monolayers were exposed to LPS and nontoxic-dose DON for 12 and 24 h to investigate the effects of DON on LPS-induced inflammatory response and tight junction variation, and specific inhibitor and CRISPR-Cas9 were used to explore the underlying mechanisms. Our results showed that nontoxic-dose DON aggravated LPS-induced cellular inflammatory response, reflecting on more significant changes of inflammatory cytokines mRNA expression, higher protein expression of NOD-like receptor protein 3 (NLRP3) and procaspase-1. Moreover, nontoxic-dose DON aggravated LPS-induced mRNA and protein expression decreased, and distribution confused of tight junction proteins. We found that DON further enhanced LPS-induced phosphorylation and nucleus translocation of p65, and expression of LC3B-II. NF- κ B inhibitor and CRISPR-Cas9-mediated knockout of LC3B attenuated the effects of combination which indicated nontoxic-dose DON aggravated LPS-induced intestinal inflammation and tight junction disorder through activating NF- κ B signaling pathway and autophagy-related protein LC3B. It further warns that ingesting low doses of mycotoxins may exacerbate the effects of intestinal pathogens on the body.

1. Introduction

Deoxynivalenol (DON) is one of the most common secondary metabolites produced by *Fusarium sp.* and mainly contaminates wheat, maize and other crops in the field and during storage (Mishra et al., 2019). DON seriously threatens the health of humans and animals, as it shows enterotoxicity, immunotoxicity and teratogenicity (Li et al., 2018a; Liao et al., 2018). Pigs are the most sensitive species to DON and intestine is the most important target organ of DON which could induce intestinal inflammation and disrupt the intestinal barrier function (Alassane-Kpembi et al., 2017; Ananthakrishnan et al., 2018). Ingestion of DON induces gut injury and inflammation, and affects growth performance of piglets (Li et al., 2018b; Pierron et al., 2018; Reddy et al., 2018). Low-dose of DON (2 μ M) exposure causes immunostimulation,

whereas high-dose of DON (16 μ M) plays as immunoinhibitory in porcine alveolar macrophage cells (PAMs) (Liu et al., 2020a). In addition, studies found that DON (3.875 mg/kg) affected developmental competence of ovaries and oocyte quality of female mouse, and 1.09 mM DON caused deformity in 50% of zebrafish larvae (Hou et al., 2014; Khezri et al., 2018). On the other hand, DON can accelerate the intestinal disease of other etiologies such as colitis induced by Dextran sulfate sodium (DSS) in adult rats (Payros et al., 2020). Pollution of DON is more common. Investigations shown that the pollution rate of DON in China is over 70% and the average pollution level is under 500 μ g/kg which is below the national hygienical standard for feeds (\leq 1000 μ g/kg, GB 13078–2017) (Ji et al., 2014; Zhao et al., 2018). According to limit standard in China, the contamination of DON is characterized by low-pollution level. *In vivo* experiments shown that ingestion of low

* Corresponding author. College of Veterinary Medicine, Nanjing Agricultural University, Nanjing, 210095, Jiangsu Province, China.

E-mail address: khhuang@njau.edu.cn (K. Huang).

<https://doi.org/10.1016/j.fct.2020.111712>

Received 15 July 2020; Received in revised form 24 August 2020; Accepted 26 August 2020

Available online 30 August 2020

0278-6915/© 2020 Elsevier Ltd. All rights reserved.

doses DON could induce anorexia, decrease of weight gain and changes in immune and reproductive systems (Cortinovis et al., 2013; Pinton et al., 2008). However, few studies have focused on the interaction between low-dose of DON and other intestinal pathogenic agents.

The gut is the most important digestive organ and the intestinal environment is complex. The gut microbiota including normal and pathogenic microorganisms as well as intakes such as nutrients and mycotoxins (Ochratoxin A [OTA], Zearalenone [ZEA] and DON) from food are the vital components in the gastrointestinal tract (Collins, 2014; Sam et al., 2017; Scarpellini et al., 2015). Changes of gut microbiota affect the development of intestinal diseases such as Irritable Bowel Syndrome (IBS), while mycotoxins can disrupt the gut microbiota balance. (Collins, 2014). Ingestion of ZEA (40 µg/kg body weight) for 6 weeks affected microbiota diversity in porcine colon contents (Piotrowska et al., 2014). The combination of ZEA and DON increased amino acid metabolism of gut microbiota, which may be detrimental (Piotrowska et al., 2014). However, DON could also increase the potential risk of intestinal pathogens. Study confirmed that Aflatoxin and Fumonisin increased Shigatoxin-producing *E. coli* (STEC) in fecal (Baines et al., 2013). DON could promote the porcine epidemic diarrhea virus (PEDV) infection though triggering p38-mediated autophagy which may suggest mycotoxin influences the prevalence of coronavirus and increases the risk of viral diseases (Liu et al., 2020b). According to the effects of mycotoxins on gut microbiota, we suspect that DON exacerbate the impact of diseases induced by intestinal pathogens. Lipopolysaccharide (LPS) is major pathogenic factor of gram-negative bacteria. As an endotoxin produced by bacteria, LPS is highly antigenic and cytotoxic which could cause significant increase of inflammatory response. *In vivo* experiment, LPS (5 mg/kg body weight) injection was used to construct acute kidney injury model in C57BL/6J male mice (Húngaro et al., 2020). *In vitro* experiments showed that treatment with 1–10 µg/mL LPS significantly improves gene expression of inflammatory markers (Bourque et al., 2018; Wu et al., 2020a; Xie et al., 2020). Studies showed that LPS (1 µg/mL) also induced intestinal barrier dysfunction, which suggests that LPS can induce intestinal injury (He et al., 2019; Wu et al., 2020b).

According to the serious harm caused by intestinal pathogenic bacteria and contamination of mycotoxins, we should pay more attention to the combination enterotoxicity caused by bacteria and mycotoxins. The aim of this study was to explore whether low-dose nontoxic DON could impact intestinal inflammation and barrier function variety induced by bacteria, and the mechanism related to these effects. In this study, the porcine intestinal cell line IPEC-J2 cell which is the common intestinal model in the study of intestinal injury was used. LPS, the main component of cell wall of gram-negative bacteria, was used to simulate the role of the gut bacteria.

2. Materials and methods

2.1. Cell culture and treatment

IPEC-J2 was cultured in DMEM/F12 medium (Gibco, USA) supplemented with 10% fetal bovine serum (FBS, Gibco, USA) and 1% penicillin-streptomycin (Gibco, USA). The cells were incubated in a 5% CO₂ cell incubator (Thermo Scientific, USA) at 37 °C. IPEC-J2 cells were seed into 96 or 6-well plates, and treated with DON and lipopolysaccharide (LPS) (1 µg/mL) for 12 or 24 h when the confluent monolayers formed. DON, LPS and dimethyl sulfoxide (DMSO) were purchased by Sigma-Aldrich (USA).

2.2. Cell viability analysis

Cell viability was measured by colorimetric 3-(4,5-dimethyl-thiazol-2-yl)-2,5-diphenyltetrazolium bromide (MTT, Sigma, USA) assay. In order to reduce the effect of LPS on cell viability, 1 µg/mL LPS, lower effective dose for activating inflammatory markers, was selected.

Monolayers of IPEC-J2 cells were cultured in 96-well plates and then treated with different concentrations of DON (0, 1, 2, 4, 8, 16 µM) and LPS (1 µg/mL) when the confluent monolayers formed. After culturing for 12 h and 24 h, MTT was added and incubated for another 4 h. Finally, removed the medium and added 150 µL DMSO to dissolve the formazan. The absorbance was measured at 490 nm using a Microplate Reader (Bio-Rad, USA).

2.3. Lactate dehydrogenase activity

The lactate dehydrogenase (LDH) activity was detected using LDH Kits (Jiancheng, China). The assay was performed as described previously (Hou et al., 2018).

2.4. Quantitative reverse transcription polymerase chain reaction (RT-qPCR)

After the corresponding treatment on cells, the total RNA was extracted by RNAiso Plus Kit (TaKaRa, China) according to the instruction. The RNA quality was assessed by the ratio of OD260/OD280. The expressions of related genes were detected using the ABI Prism Step One Plus detection system (Applied Biosystems, USA). The expression levels of mRNA were calculated by 2^{-ΔΔCT} method and normalized with the housekeeping gene β-actin. The reverse transcription used Prime Script II 1st Strand cDNA Synthesis Kit (TaKaRa, China) and real-time PCR was performed by SYBR Premix Ex Taq II (TaKaRa, China) and ABI 7500 real-time PCR system (Applied Biosystems, USA). The primers used were synthesized by Sangon Biotech (Shanghai, China) (Table 1).

2.5. Western blotting analysis

After corresponding treatment, monolayers of IPEC-J2 cells in 6-well plates were washed 3 times with ice-cold PBS. After washing, RIPA lysis buffer containing 1% PMSF protease inhibitor was added. Cells were broken by an ultrasonic cell disruptor, and the supernatant was collected after centrifuging at 4 °C and 12000 rpm for 15 min. The concentration of protein was detected by BCA Protein Assay Kit (Beyotime, China). The next progress of western blotting was performed as described previously (Su et al., 2019). Proteins were detected by specific primary antibodies: ZO-1 (AF5145, 1:1000, Affinity, China), Occludin (ab167161, 1:1000, Abcam, UK), NLRP3 (DF7438, 1:500, Affinity, China), procaspase-1 (AF5418, 1:500, Affinity, China), p65 (AF1234, 1:1000, Beyotime, China), pp65 (AF5875, 1:1000, Beyotime, China), IκB-α (AF2176, 1:1000, Beyotime, China), LC3B (L8918, 1:1000, Sigma, USA). The secondary antibody was Anti-rabbit IgG antibody (#7074, 1:10000, CST, USA).

Table 1
Gene sequence.

Target gene	Accession number	Primer sequence (5'-3')	Tm (°C)
TNF-α	NM_214022.1	F: GCCCTTCCACCAACGTTTTC	57.4
		R: CAAGGGCTCTTGATGGCAGA	57.8
IL-6	NM_214399.1	F: CCTCTCCGGACAAAACCTGAA	57.5
		R: TCTGCCAGTACCTCCTTGCT	57.3
TGF-β	XM_021093503.1	F: GGACCTTATCCTGAATGCCTT	57.6
		R: TAGGTTACCACTAGCCACAAT	56.7
ZO-1	XM_021098848.1	F: ATGAGCAGGTCCCCTCCCAAG	62.6
		R: GGCGGAGGCAGCGGTTTG	64.2
Occludin	XM_005672522.3	F: GACAGACTACACAACCTGGCGG	58.5
		R: TGTACTCCTGCAGGCCACTG	60.2
Claudin-1	NM_001244539.1	F: CCATCGTCAGCACGCCACTG	62.5
		R: CGACACGCAGGACATCCACAG	61.5
β-actin	XM_021086047.1	F: CTGGCGCATCCAGAAACT	58.9
		R: AGGGCCGTGATCTCCTCTG	59.8

2.6. Immunofluorescence

Monolayers of IPEC-J2 cells were cultured on glass coverslips which were placed in 12-well plates. Cells were fixed in 4% paraformaldehyde at 4 °C for 20 min after washing 3 times using PBS, and then 0.2% Triton X-100 was added for 20 min and blocked with 1% bovine serum albumin (BSA, Solarbio, China) at 37 °C for 1 h. Next, cells were incubated using specific primary antibody at 4 °C overnight, and then incubated with secondary FITC-labeled antibody (1:100, Solarbio, China). Finally, cell nuclei were stained with DAPI (Beyotime, China) at room temperature for 5 min. Images were captured using laser scanning confocal microscope (Carl Zeiss, Germany). Primary antibody was ZO-1 (13663S, 1:300, CST, USA).

2.7. LC3B^{-/-} IPEC-J2 cells construction by CRISPR/Cas9 system

The small guide RNAs (sgRNAs) were designed using Breaking-Cas online tool and synthesized (Invitrogen). The sgRNA was cloned pCas-Puro-U6 plasmid and the pCas-Puro-U6 plasmid Linear was obtained using the BbsI restriction enzyme (Thermo Fisher Scientific, USA). The plasmids containing sgRNA were transfected into IPEC-J2 cells with GeneTran III (Biomiga, USA) for 48 h, and then the transfected cells were selected using 5 µg/mL of puromycin. The selected cells were subjected to serial dilutions in 96-well plate to obtain a single cell colony. Each single colony was picked and expanded after colony formation. Genomic DNA was extracted from individual clones and sequenced to confirm the specificity of targeting.

2.8. Statistical analysis

The experimental data were analyzed using SPSS 19.0 for statistical analysis. Data were presented as the mean ± SEM. All experiments were

performed at least three times. One-way analysis of variance (ANOVA) was used to analyze the differences for multiple groups. */# indicated $P < 0.05$ and **/## indicated $P < 0.01$.

3. Results

3.1. Cytotoxic effects of DON combined with LPS in IPEC-J2 cell monolayers

The cytotoxic effects of DON combined with LPS in IPEC-J2 monolayers were tested by MTT assay and LDH activity assay after treatments of DON (0, 1, 2, 4, 8, 16 µM) and LPS (1 µg/mL) for 12 h and 24 h, and the results were shown in Fig. 1. The result of MTT assay (Fig. 1A and C) demonstrated that cell viability was decreased with the increase of the concentration of DON. 8 µM or higher concentration of DON combined with LPS caused significant decrease of cell viability. The result of LDH assay was shown in Fig. 1B and D which demonstrated that DON promoted the release of LDH in a dose-dependent manner which reflected similar results with MTT assay. Thus, non-lethal concentration of DON (2 µM) combined with LPS (1 µg/mL) was selected for subsequent experiments.

3.2. Nontoxic-dose DON aggravated inflammation induced by LPS in IPEC-J2 cell monolayers

To investigate the inflammatory effects of LPS combined with nontoxic-dose DON in IPEC-J2 monolayers, cells were exposed to DON and LPS for 12 and 24 h after the confluent monolayers formed, and pro-inflammatory cytokines (IL-6 and TNF-α) and anti-inflammatory cytokine (TGF-β) were assessed by RT-qPCR. The expression of IL-6 and TNF-α mRNA in DON-LPS group were significantly increased in the 12 h and 24 h compared with that in LPS group, which were also significantly

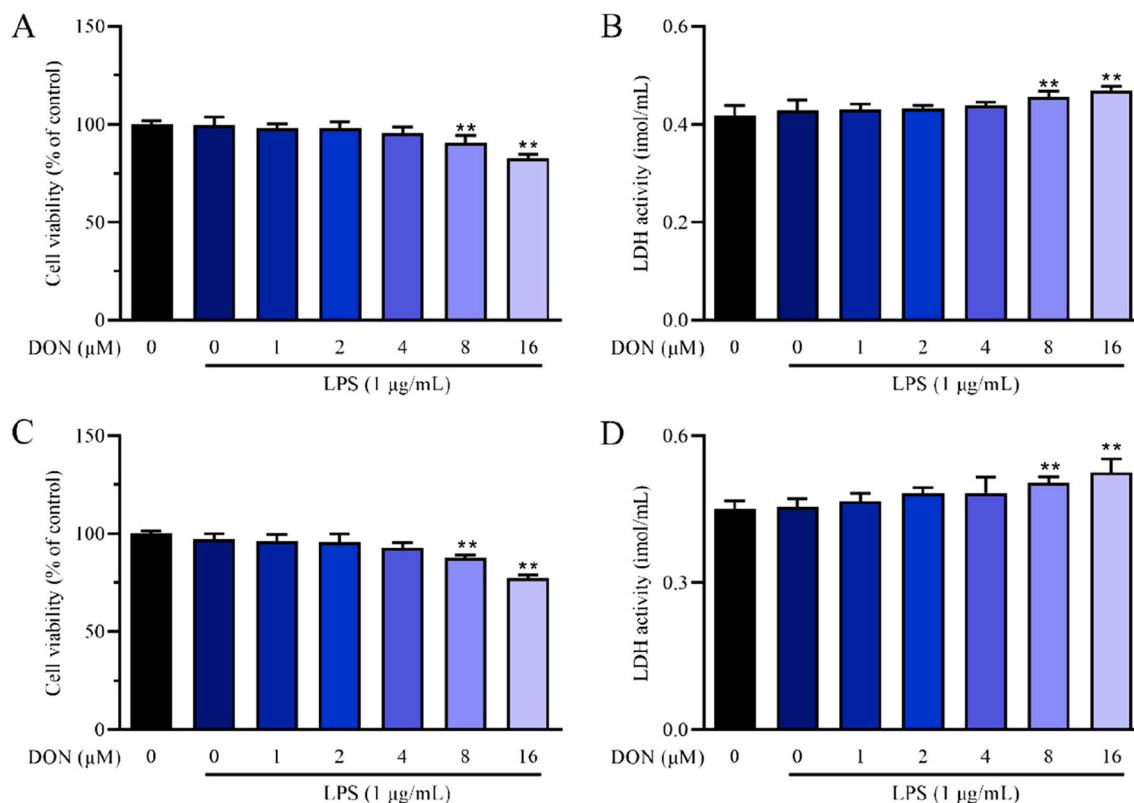


Fig. 1. Cytotoxic effect of DON combined with LPS for 12 h and 24 h of IPEC-J2 cell monolayers. Monolayers of IPEC-J2 cells were exposed with different concentrations of DON (0, 1, 2, 4, 8, 16 µM) and LPS (1 µg/mL) for 12 h and 24 h. The cell viability was assessed by MTT assay (A for 12 h and C for 24 h) and LDH activity assay (B for 12 h and D for 24 h) respectively. Data were presented as mean ± SEM (n = 6). * $P < 0.05$ and ** $P < 0.01$ vs. control group.

higher than that in control and DON group ($P < 0.05$) (Fig. 2). These results suggested that nontoxic-dose DON could aggravate the inflammation induced by LPS in IPEC-J2 cells.

3.3. Nontoxic-dose DON further increased protein expression of NLRP3 and procaspase-1 induced by LPS in IPEC-J2 cell monolayers

To evaluate the effects of DON and/or LPS on NLRP3 and procaspase-1, the related protein expression of IPEC-J2 monolayers after corresponding treatment was measured by western blotting. As shown in Fig. 3, exposure to DON for 24 h didn't affect the protein expression level of NLRP3 and procaspase-1, while the addition of LPS significantly increased ($P < 0.05$) the protein expression of NLRP3 and procaspase-1 compared with control and DON group. In comparison with the LPS group, the combination of DON and LPS further increased NLRP3, while the expression of procaspase-1 also increased but not significantly. Therefore, nontoxic-dose DON could further promote LPS-induced protein expression level of NLRP3 and procaspase-1 in IPEC-J2 monolayers, which may reflect the activation of NLRP3 inflammasome.

3.4. Nontoxic-dose DON aggravated tight junction disorder induced by LPS in IPEC-J2 cell monolayers

To investigate the intestinal epithelial barrier function changes induced by DON and/or LPS, the relative mRNA and protein expression and of tight junction was assessed by qRT-PCR and western blotting respectively. The distribution of tight junction protein ZO-1 was measured using immunofluorescence respectively after cells confluent monolayers formed. As shown in Fig. 4A and B, treatment with LPS for 12 h and 24 h significantly reduced the mRNA expression of tight junction (ZO-1, Occludin and Claudin-1). The expression of ZO-1 and Occludin mRNA but not Claudin-1 decreased significantly in DON/LPS group compared with LPS group. Then the protein expression of ZO-1 and Occludin was assessed which showed a down-regulation after treatment of LPS and DON-LPS for 12 and 24 h, and DON combined with LPS showed more significant decrease ($P < 0.01$) compared with LPS treatment alone (Fig. 4C and D). Compared with control and DON group, the distribution of ZO-1 was more disordered in LPS and DON-LPS groups, and the disorder of DON-LPS group was the most serious (Fig. 4E). These suggested that nontoxic-dose DON could aggravate LPS-induced damage to tight junction expression and structure.

3.5. Role of NF- κ B (p65) signaling pathway in nontoxic-dose DON aggravated inflammation and tight junction disorder induced by LPS in IPEC-J2 cell monolayers

The aforementioned results have confirmed that DON combined with LPS could lead to inflammation and tight junction disorder. Whether NF-

κ B (p65) signaling pathway, one of the main regulators on inflammation and immune response, is involved in the above reactions remains to be investigated. The effects of DON and/or LPS on NF- κ B signaling pathway in IPEC-J2 cells were shown in Fig. 5A, after corresponding treatment for 24 h. DON alone didn't activate the NF- κ B while LPS and DON/LPS treatment significantly promoted the phosphorylation of p65 and inhibited the protein expression of I κ B- α (Fig. 5A). Meanwhile, we tested the distribution of p65 protein in IPEC-J2 cells by immunofluorescence assay and found that the combination of LPS and DON promoted p65 translocation into the nucleus (Fig. 5B). These results suggested that NF- κ B (p65) signaling pathway was activated after treatment with DON combined with LPS in IPEC-J2 cells.

To address whether NF- κ B signaling pathway plays a key role in inflammatory reaction and tight junction disorder induced by DON combined with LPS, BAY 11-7082 (Beyotime, China), a common NF- κ B inhibitor, was used to inhibit NF- κ B signaling pathway. Before corresponding treatment, the confluent monolayer cells were pretreated with 2.5 μ M BAY for 2 h. As shown in Fig. 5C and D, the addition of BAY 11-7082 reversed the inflammatory reaction and the expression of NLRP3 and procaspase-1 protein was also inhibited. In addition, tight junction protein down-trend induced by the union of DON and LPS was also eased (Fig. 5E). These results verified that NF- κ B signaling pathway played a regulatory role in inflammatory reaction and tight junction dysfunction induced by LPS combined with nontoxic-dose DON in IPEC-J2 monolayers.

3.6. Role of LC3B in inflammation and tight junction induced by LPS combined with nontoxic-dose DON in IPEC-J2 cell monolayers

To further explore whether treatment with DON and LPS induces autophagy in IPEC-J2 cells, the expression of autophagy-related protein LC3B was detected by western blotting after corresponding treatment. As shown in Fig. 6A, DON combined with LPS led to a significant increase ($P < 0.01$) in LC3B-II expression. These results indicated that treatment with DON and LPS could promote LC3B-II expression in IPEC-J2 confluent monolayer.

According to the above results, treatment of DON and LPS could increase LC3B-II level in IPEC-J2 cells. To further investigate the role of LC3B in this cellular reaction, knockout cell line LC3B^{-/-} IPEC-J2 cell was constructed by CRISPR/Cas9 system (Fig. 6B). The expression of inflammatory cytokines in LC3B^{-/-} IPEC-J2 cells was different from that in wild type (WT) cells, mainly reflected in the increase of IL-6 and TNF- α mRNA levels, and the decrease of TGF- β mRNA level which suggested that the inflammatory responses states of two cell lines were not consistent (Fig. 6C). However, the mRNA expression of IL-6 and TGF- β in LC3B^{-/-} IPEC-J2 cells was significantly reversed while TNF- α was not compared with IPEC-J2 cells after both treatment with DON and LPS (Fig. 6C). LC3B knockout also inhibited the elevated expression of

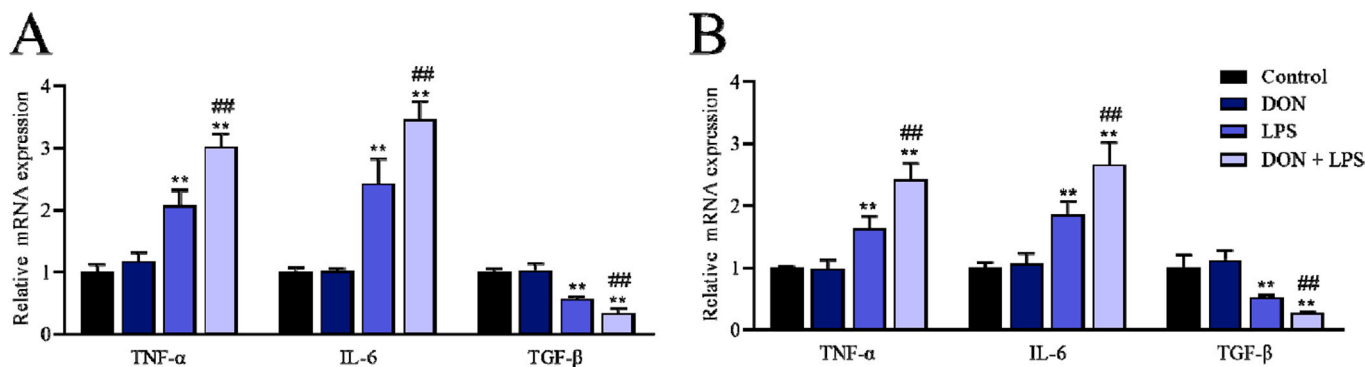


Fig. 2. Effects of LPS combined with nontoxic-dose DON on inflammatory cytokines of IPEC-J2 cell monolayers. IPEC-J2 cells were exposed to DON (2 μ M) and/or LPS (1 μ g/mL) for 12 h and 24 h. The expression of TNF- α , IL-6 and TGF- β mRNA was measured by RT-qPCR after corresponding treatments for 12 h (A) and 24 h (B) respectively. Data were presented as mean \pm SEM (n = 3). * $P < 0.05$ and ** $P < 0.01$ vs. control group. # $P < 0.05$ and ### $P < 0.01$ vs. LPS group.

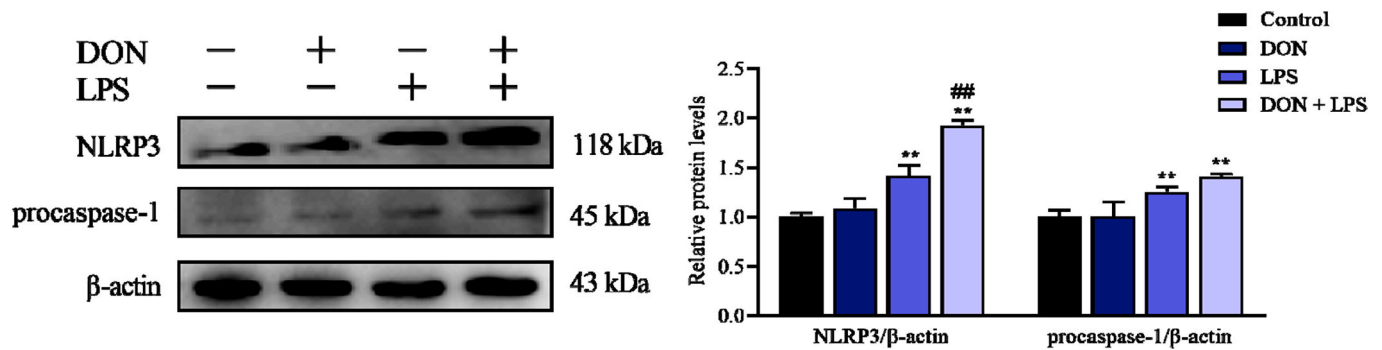


Fig. 3. Effects of LPS combined with nontoxic-dose DON on protein expression of NLRP3 and procaspase-1 of IPEC-J2 cell monolayers. After corresponding treatment using DON and LPS for 24 h, the protein expression of NLRP3 and procaspase-1 of IPEC-J2 cells was measured by western blotting. Data were presented as mean \pm SEM (n = 3). * P < 0.05 and ** P < 0.01 vs. control group. # P < 0.05 and ## P < 0.01 vs. LPS group.

NLRP3 and procaspase-1 protein after DON and LPS treatment (Fig. 6D). At the same time, the expression of tight junction protein ZO-1 and Occludin was not affected by treatment with LPS and DON in LC3B^{-/-} IPEC-J2 cells (Fig. 6E). These results suggested that LC3B knockout could effectively alleviate the damage of DON and LPS combined application to IPEC-J2 cells, which indicated that LC3B or autophagy played an important regulatory role in inflammatory reaction and epithelial barrier dysfunction induced by LPS combined with nontoxic-dose DON in IPEC-J2 cell monolayers.

4. Discussion

Deoxynivalenol (DON), as a wide-spread contamination mycotoxin, widely exists in feed and seriously threatens animal health. DON has been reported to induce inflammation both *in vivo* and *in vitro* (Peng et al., 2019; Yu et al., 2019). According to previous studies, toxic dose of DON (over 0.5 μ g/mL) mainly induced inflammation in the intestinal epithelial cells (Kang et al., 2019; Li et al., 2018b). Acute high doses of DON (over 2.0 mg/kg feed) could cause diarrhea, vomiting and hemorrhage in animals, whereas low doses of DON (approximately 1 mg/kg feed) induced anorexia, decrease of weight gain and changes in immune and reproductive systems (Cortinovis et al., 2013; Gerez et al., 2017; Pinton et al., 2008). In fact, ingestion of low-dose DON (under 0.5 mg/kg feed) in animals is more common according to the contamination of DON (Wall-Martinez et al., 2019; Zhao et al., 2018). Intestine, the main target organ of DON, is a complex environment in which germ and mycotoxins interact. Chen et al. suggested that nontoxic OTA (4 μ M) could promote DON-induced (4 μ M) intestinal barrier dysfunction in IPEC-J2 cells (Ying et al., 2019). Wageha et al. have found that DON (5 and 10 mg/kg feed) could facilitate the translocation of enteric microorganisms such as *E. coli* to extra-intestinal organs in broiler chickens (Awad et al., 2019). However, the interaction and its mechanism between germ and DON are still unclear.

In this study, we focused on the effects of low-dose DON on bacteria-induced intestinal inflammation and barrier function dysfunction. Endotoxin LPS from *E. coli* was used to simulate the role of intestinal gram-negative bacteria, and the porcine intestinal cell line IPEC-J2 was used to evaluate the varieties on intestinal inflammation and barrier function.

In the present study, the nontoxic concentration of DON was selected using MTT assay and LDH activity assay. *In vitro* experiments shown that LPS (1–10 μ g/mL) can induce inflammatory response, and 1 μ g/mL LPS is the common dose used to induce barrier dysfunction in intestinal epithelial cells. Nontoxic concentration of DON combined with LPS was similar with DON treatment alone according to previous study, which showed 1 μ g/mL LPS didn't affect the toxicity of DON (Ying et al., 2019). So, 1 μ g/mL LPS was selected and treatment with combination of DON (0–4 μ M) and LPS (1 μ g/mL) showed no cytotoxic to monolayers IPEC-J2 cells for 12 h and 24 h (Fig. 1). Therefore, 0–4 μ M DON was considered

as nontoxic dose on the basic treatment with LPS (1 μ g/mL), and the nontoxic concentration (2 μ M DON and 1 μ g/mL LPS) was selected for subsequent study. The mRNA expression of pro-inflammatory cytokines (IL-6 and TNF- α) in IPEC-J2 were significantly increased, whereas anti-inflammatory cytokine TGF- β was decreased after LPS treatment alone for 12 or 24 h. The increasing or decreasing trend of related cytokines were more significant when cells were co-exposed to DON and LPS (Fig. 2). These results suggested that the addition of nontoxic-dose DON could enhance the inflammatory response induced by LPS in IPEC-J2 cells, which were similar with earlier research that LPS combined with DON could induce a certain up-regulation of the pro-inflammatory response in the duodenum of broiler chickens (Lucke et al., 2018). The NLRP3 inflammasome, a member of innate immune receptor NLR family which execute cellular inflammation processes, is expressed in gut epithelial cells and plays an important role in intestinal inflammation and infectious enteritis (Hirota et al., 2011; Zmora et al., 2017). Ge et al. found that the activation of NLRP3 inflammasome induced the production of proinflammatory cytokines (Ge et al., 2017). In the present study, the protein expression of NLRP3 and procaspase-1 was increased induced by LPS, which was a common activator of NLRP3 inflammasome (Wang et al., 2019a). With the addition of nontoxic-dose DON, NLRP3 expression level but not procaspase-1 was significantly increased which demonstrated the further activation of NLRP3 was induced by nontoxic-dose DON on the basis of LPS treatment (Fig. 3). Considering the increase expressions of the important components of NLRP3 inflammasome, we estimated that the activation of NLRP3 inflammasome is involved in nontoxic-dose DON exacerbating the LPS-induced inflammatory response.

The intestinal mucosa constitutes an essential barrier which is directly related to health of human and animals, and DON has been reported to injure the intestinal barrier function according to many studies (De Walle et al., 2010; Konig et al., 2016; Peyman et al., 2014; Romero et al., 2016). Tight junction (TJ) is the main connection form between intestinal epithelial cells, and plays an important role in maintaining intestinal epithelial mechanical barrier (Zeisel et al., 2019). Tight junction proteins, including ZO-1, Occludin and Claudins, are directly related to the function of tight junction barrier (Mir et al., 2016; Wong et al., 2017; Xiao et al., 2016). In the present study, ZO-1 and Occludin which could reflect the diversification of intestinal epithelial barrier were measured using western blotting and immunofluorescence to explore the expression and distribution of tight junction protein. We observed that nontoxic-dose DON treatment alone had no significant impact on the protein expression of ZO-1 and Occludin, and the distribution of ZO-1 (Fig. 4). However, nontoxic-dose DON exacerbated the decreasing mRNA and protein expression of ZO-1 and Occludin induced by LPS treatment while expression of Claudin-1 mRNA had no significant declined (Fig. 4A–D). Meanwhile, the disordered distribution of ZO-1 was more serious after co-exposed with DON and LPS compared with that induced by LPS alone (Fig. 4E). These results showed that

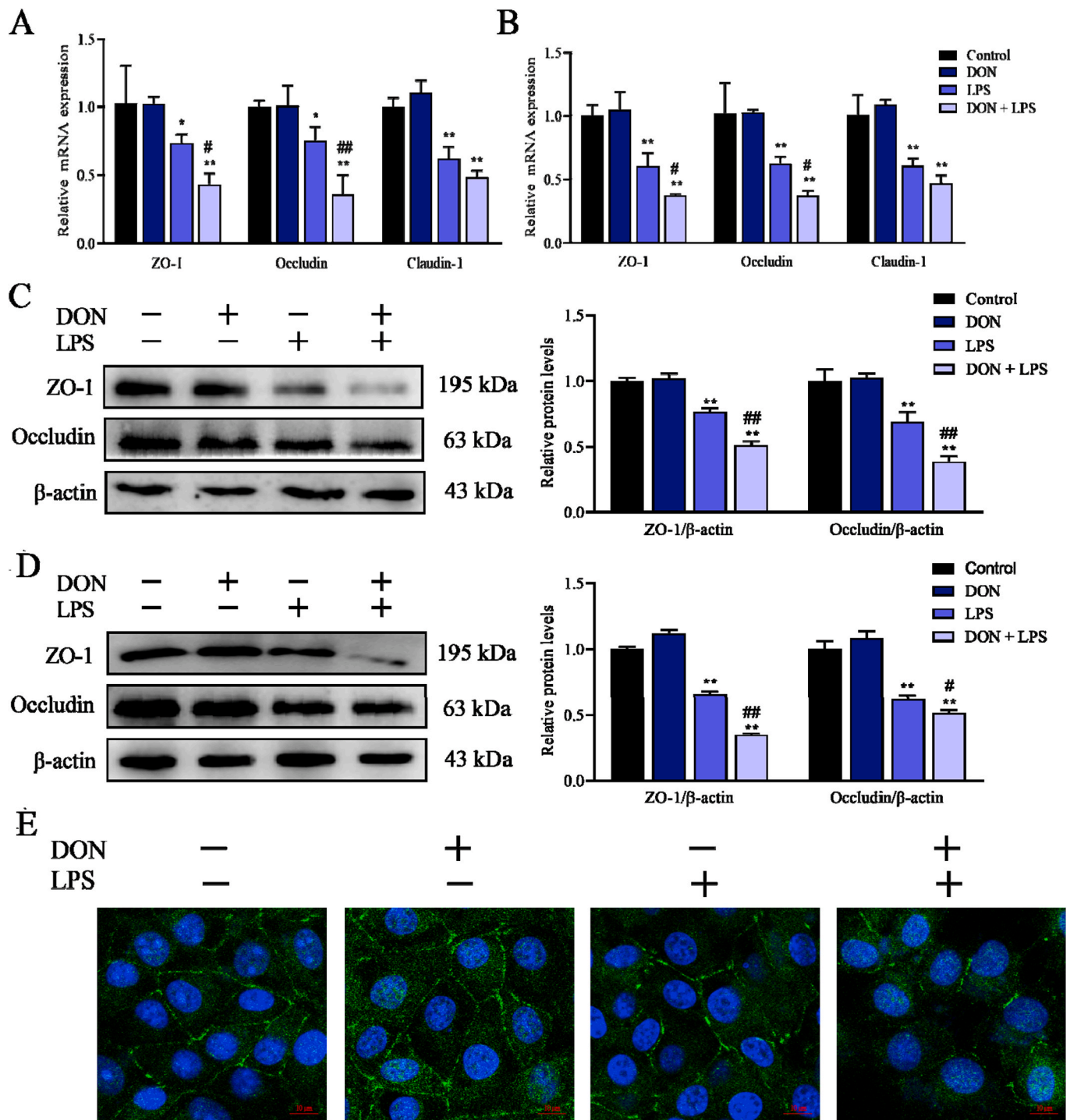


Fig. 4. Effects of LPS combined with nontoxic-dose DON on expression and distribution of tight junction proteins of IPEC-J2 cell monolayers. After corresponding treatment using DON and LPS, the mRNA expression of ZO-1, Occludin and Claudin-1 was assessed using qRT-PCR (A for 12 h and B for 24 h). The expression of tight junction protein (ZO-1 and Occludin) of IPEC-J2 cells was measured by western blotting (C for 12 h and D for 24 h). After treatment for 24 h, the distribution of ZO-1 (green) was measured by immunofluorescence (DAPI, nucleus, blue) (E). Data were presented as mean ± SEM (n = 3). **P* < 0.05 and ***P* < 0.01 vs. control group. #*P* < 0.05 and ##*P* < 0.01 vs. LPS group. (For interpretation of the references to color in this figure legend, the reader is referred to the Web version of this article.)

nontoxic-dose DON aggravated intestinal epithelial barrier dysfunction induced by LPS which were consistent with earlier reports that low doses of mycotoxins could intensify the effects induced by other stimulants (Qian et al., 2017; Ying et al., 2019).

Next, we further studied the mechanism of the above phenomenon that nontoxic-dose DON could aggravated LPS-induced intestinal inflammation and barrier dysfunction in IPEC-J2 cell monolayers. Many

studies have reported that mycotoxins could regulate inflammatory cytokines through regulating nuclear factor-κB (NF-κB) signaling pathway (Shao et al., 2019; Sugiyama et al., 2016; Wang et al., 2019b; Zmora et al., 2017). In addition, NF-κB has been reported to regulate the tight junction barrier and NLRP3 inflammasome response to some extracellular stimuli (Al-Sadi et al., 2010; Guo et al., 2019; Zmora et al., 2017). Therefore, we speculated that NF-κB signaling pathway may be

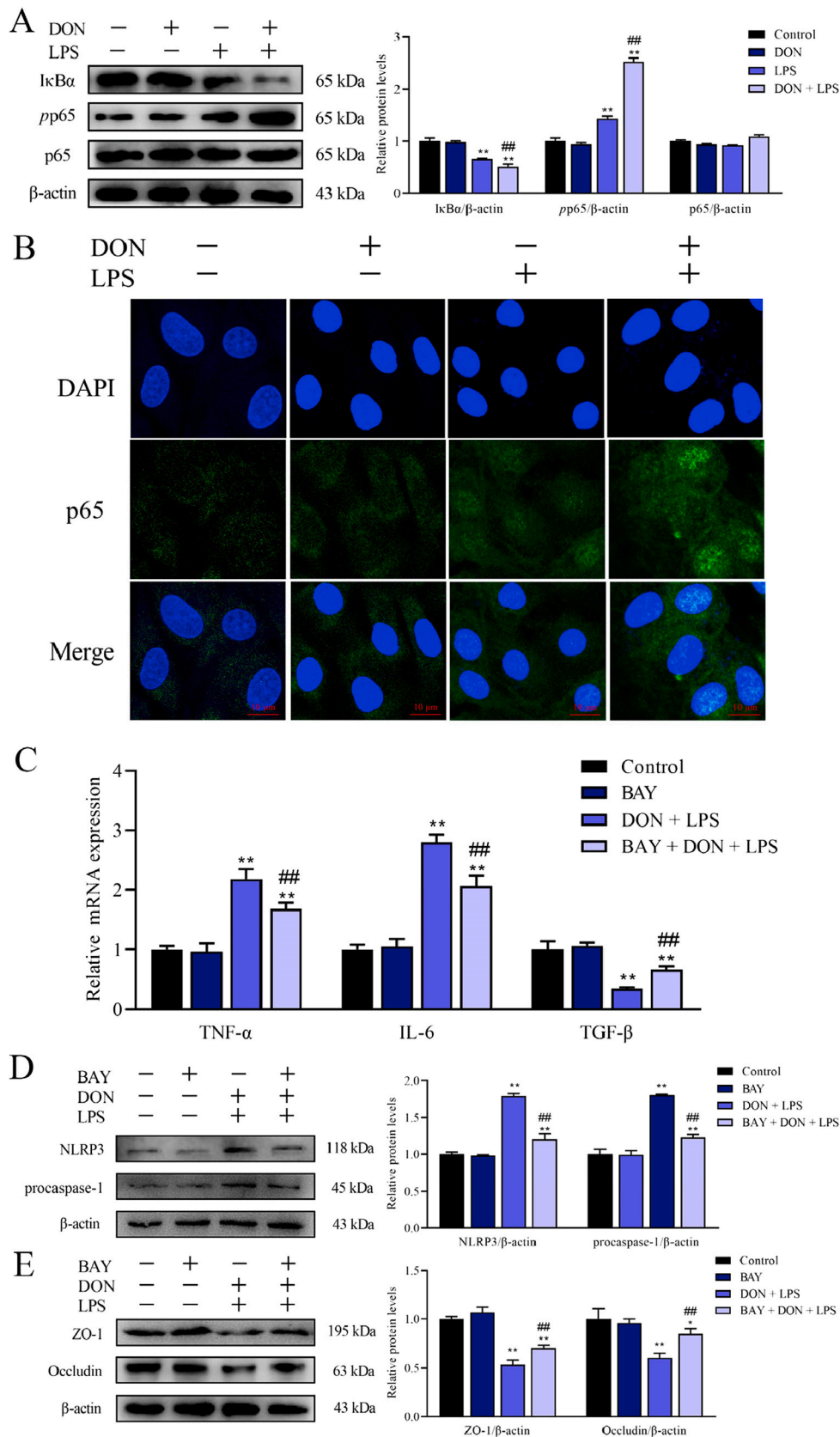


Fig. 5. Role of NF- κ B in inflammation and intestinal epithelial barrier dysfunction of IPEC-J2 monolayers induced by LPS combined with nontoxic-dose DON. After corresponding treatment using DON and LPS, the expression of I κ B- α , pp65 and p65 protein was determined by western blotting (A). The distribution of p65 inside and outside the nucleus was measured by immunofluorescence (B). Cells were immunostained with p65 (green) antibody and DAPI (nucleus, blue). After addition of inhibitor BAY 11-7082, the expression of TNF- α , IL-6 and TGF- β was measured by RT-qPCR (C) and the expression of NLRP3 (D) and tight junction protein (ZO-1 and Occludin) (E) was measured by western blotting. * $P < 0.05$ and ** $P < 0.01$ vs. control group. # $P < 0.05$ and ## $P < 0.01$ vs. LPS group. (For interpretation of the references to color in this figure legend, the reader is referred to the Web version of this article.)

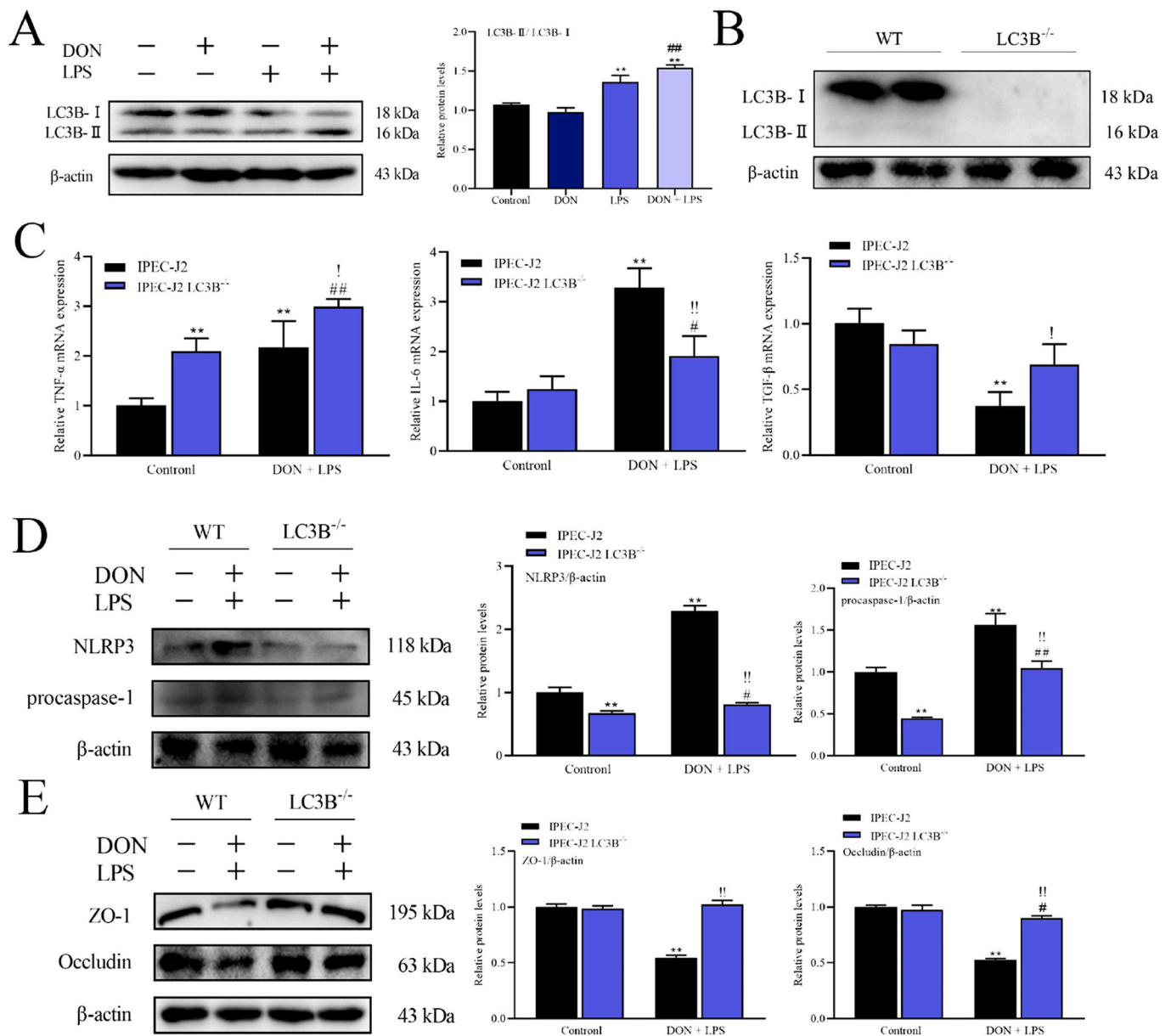


Fig. 6. Role of LC3B in inflammation and intestinal epithelial barrier dysfunction of IPEC-J2 cell monolayers induced by nontoxic-dose DON and LPS. After corresponding treatment using DON and LPS, the expression of LC3B was determined by western blotting (A). LC3B^{-/-} IPEC-J2 cell was constructed by CRISPR/Cas9 system (B). The expression of TNF-α, IL-6 and TGF-β mRNA was measured by RT-qPCR (C), and the protein expression of NLRP3 (D) and tight junction protein (ZO-1 and Occludin) (E) was measured by western blotting after corresponding treatment in IPEC-J2 cells and LC3B^{-/-} IPEC-J2 cells. **P* < 0.05 and ***P* < 0.01 vs. IPEC-J2 control group. #*P* < 0.05 and ##*P* < 0.01 vs. IPEC-J2 LC3B^{-/-} control group. !*P* < 0.05 and !!*P* < 0.01 vs. IPEC-J2 DON + LPS group.

associated with the aggravating effects of inflammation and barrier dysfunction induced by DON and LPS. Firstly, we confirmed that nontoxic-dose DON could further activate NF-κB (p65) signaling pathway induced by LPS, and induce migration of p65 into the nucleus (Fig. 5A and B). Then, the intestinal inflammation and tight junction disorder were relieved after the addition of NF-κB inhibitor BAY 11-7082 (Fig. 5C and E), which proved that NF-κB signaling pathway played a regulatory role in nontoxic-dose DON aggravated LPS-induced intestinal inflammation and barrier dysfunction. However, intestinal inflammation and barrier function did not return to normal level. So, we speculated that NF-κB signaling pathway is not the only pathway to regulate these varieties.

Autophagy is a critical cellular process which has been implicated in a variety of pathogenic process of mycotoxins (Islam et al., 2013; Qian et al., 2017). Numerous studies have highlighted the critical role of

autophagy in inflammatory cytokine responses (Aden et al., 2018; Macias-Ceja et al., 2017). Autophagy is also critical for the development and function of intestinal epithelial cells (Matsuzawa-Ishimoto et al., 2017; Pott et al., 2018). However, autophagy may have different phenotypic effects in each cell type in intestinal homeostasis and inflammatory bowel diseases (Lassen and Xavier, 2018). Considering the intertwined relationship between autophagy, inflammation and intestinal injury, we suspected whether autophagy is involved in the regulation of cellular reaction induced by DON and LPS in IPEC-J2 cells. In this study, we focused on one of autophagy-related proteins LC3B and an increasing expression level of LC3B-II was observed after treatment with LPS or DON/LPS in IPEC-J2 cell monolayers (Fig. 6A). Li et al. described that inhibition of autophagy could reduce intestinal injury induced by I/R (Li et al., 2019). And Yamoto et al. found that inhibiting autophagy may be a new strategy for treating intestinal diseases (Yamoto et al.,

2019). To further investigate the role of LC3B, we constructed LC3B^{-/-} IPEC-J2 cell lines (Fig. 6B). As shown in Fig. 6C, knock-out LC3B could relieve the inflammatory response. Meanwhile, the protein expression of NLRP3 and procaspase-1 was also decreased on LC3B^{-/-} IPEC-J2 after corresponding treatment compared with WT cells (Fig. 6D). In addition, knock-out LC3B basically eliminated the impact on the tight junction induced by LPS combined with nontoxic-dose DON in IPEC-J2 cell monolayers (Fig. 6E). Taken together, the results demonstrated that the accumulation of LC3B played a negative regulatory role in nontoxic-dose DON aggravated LPS-induced intestinal inflammation and barrier dysfunction.

5. Conclusion

In conclusion, our study demonstrated that nontoxic-dose DON could aggravate the cellular inflammation response and tight junction dysfunction induced by LPS in IPEC-J2 cell monolayers. We also confirmed that NF- κ B (p65) signaling pathway and autophagy-related protein LC3B played a regulatory role in nontoxic-dose DON aggravated LPS-induced intestinal inflammation and tight junction disorder. Therefore, these findings indicate nontoxic-dose mycotoxins could exacerbate the negative effects of intestinal bacteria and increase vigilance against low concentration of mycotoxin contamination.

CRediT authorship contribution statement

Lei Ge: Investigation, Data curation, Writing - original draft, Writing - review & editing. **Ziman Lin:** Investigation, Data curation. **Guannan Le:** Investigation, Data curation. **Lili Hou:** Investigation, Data curation. **Xinru Mao:** Investigation, Data curation. **Shuiping Liu:** Investigation, Data curation. **Dandan Liu:** Investigation, Data curation. **Fang Gan:** Conceptualization, Methodology, Supervision, Writing - review & editing. **Kehe Huang:** Conceptualization, Methodology, Supervision, Writing - review & editing.

Declaration of competing interest

The authors declare that they have no known competing financial interests or personal relationships that could have appeared to influence the work reported in this paper.

Acknowledgments

This work was funded by the National Science Foundation of China (31772811), the Priority Academic Program Development of Jiangsu Higher Education Institutions (Jiangsu, China) and the Postgraduate Research & Practice Innovation Program of Jiangsu Province (SJCS19_0157).

Abbreviations

LPS	lipopolysaccharides
DON	deoxynivalenol
OTA	Ochratoxin A
ZEA	Zearalenone
IPEC-J2	the porcine intestinal epithelial cell
TNF- α	tumor necrosis factor-alpha
IL-6	interleukin-6
TGF- β	transforming growth factor-beta
β -actin	beta-actin
NLRP3	NOD-like receptor protein 3
ZO-1	zona occludens-1
FBS	fetal bovine serum
NF- κ B	nuclear factor-kappa b
MTT	3-(4,5-dimethyl-thiazol-2-yl)-2,5-diphenyltetrazolium bromide;

LDH	lactate dehydrogenase
DMSO	dimethyl sulfoxide;
BSA	bovine serum albumin
DAPI	4',6-diamidino-2-phenylindole
ANOVA	one-way analysis of variance
SEN	standard error of mean

Appendix A. Supplementary data

Supplementary data to this article can be found online at <https://doi.org/10.1016/j.fct.2020.111712>.

References

- Aden, K., et al., 2018. ATG16L1 orchestrates interleukin-22 signaling in the intestinal epithelium via cGAS-STING. *J. Exp. Med.* 215, 2868–2886. <https://doi.org/10.1084/jem.20171029>.
- Al-Sadi, R., et al., 2010. IL-1beta-induced increase in intestinal epithelial tight junction permeability is mediated by MEKK-1 activation of canonical NF-kappaB pathway. *Am. J. Pathol.* 177, 2310–2322. <https://doi.org/10.2353/ajpath.2010.100371>.
- Alassane-Kpembi, I., et al., 2017. Co-exposure to low doses of the food contaminants deoxynivalenol and nivalenol has a synergistic inflammatory effect on intestinal explants. *Arch. Toxicol.* 91, 2677–2687. <https://doi.org/10.1007/s00204-016-1902-9>.
- Ananthkrishnan, A.N., et al., 2018. Environmental triggers in IBD: a review of progress and evidence. *Nat. Rev. Gastroenterol. Hepatol.* 15, 39–49. <https://doi.org/10.1038/nrgastro.2017.136>.
- Awad, W.A., et al., 2019. Feeding of deoxynivalenol increases the intestinal paracellular permeability of broiler chickens. *Arch. Toxicol.* 93, 2057–2064. <https://doi.org/10.1007/s00204-019-02460-3>.
- Baines, D., et al., 2013. Aflatoxin, fumonisin and Shiga toxin-producing *Escherichia coli* infections in calves and the effectiveness of Celmanax(R)/Dairyman's Choice applications to eliminate morbidity and mortality losses. *Toxins* 5, 1872–1895. <https://doi.org/10.3390/toxins5101872>.
- Bourque, C., et al., 2018. H(2)S protects lipopolysaccharide-induced inflammation by blocking NFkB transactivation in endothelial cells. *Toxicol. Appl. Pharmacol.* 338, 20–29. <https://doi.org/10.1016/j.taap.2017.11.004>.
- Collins, S.M., 2014. A role for the gut microbiota in IBS. *Nat. Rev. Gastroenterol. Hepatol.* 11, 497–505. <https://doi.org/10.1038/nrgastro.2014.40>.
- Cortinovis, C., et al., 2013. Fusarium mycotoxins: effects on reproductive function in domestic animals—a review. *Theriogenology* 80, 557–564. <https://doi.org/10.1016/j.theriogenology.2013.06.018>.
- De Walle, J.V., et al., 2010. Deoxynivalenol affects in vitro intestinal epithelial cell barrier integrity through inhibition of protein synthesis. *Toxicol. Appl. Pharmacol.* 245, 291–298. <https://doi.org/10.1016/j.taap.2010.03.012>.
- Ge, H., et al., 2017. Rhein attenuates inflammation through inhibition of NF-kappaB and NALP3 inflammasome in vivo and in vitro. *Drug Des. Dev. Ther.* 11, 1663–1671. <https://doi.org/10.2147/DDDT.S133069>.
- Gerez, J.R., et al., 2017. Deoxynivalenol induces toxic effects in the ovaries of pigs: an ex vivo approach. *Theriogenology* 90, 94–100. <https://doi.org/10.1016/j.theriogenology.2016.10.023>.
- He, C., et al., 2019. Vitamin A inhibits the action of LPS on the intestinal epithelial barrier function and tight junction proteins. *Food Funct* 10, 1235–1242. <https://doi.org/10.1039/c8fo01123k>.
- Hirota, S.A., et al., 2011. NLRP3 inflammasome plays a key role in the regulation of intestinal homeostasis. *Inflamm. Bowel Dis.* 17, 1359–1372. <https://doi.org/10.1002/ibd.21478>.
- Hou, Y.J., et al., 2014. Oocyte quality in mice is affected by a mycotoxin-contaminated diet. *Environ. Mol. Mutagen.* 55, 354–362. <https://doi.org/10.1002/em.21833>.
- Hou, L., et al., 2018. Immunotoxicity of ochratoxin A and aflatoxin B1 in combination is associated with the nuclear factor kappa B signaling pathway in 3D4/21 cells. *Chemosphere* 199, 718–727. <https://doi.org/10.1016/j.chemosphere.2018.02.009>.
- Húngaro, T.G.R., et al., 2020. Physical exercise exacerbates acute kidney injury induced by LPS via toll-like receptor 4. *Front. Physiol.* 11, 768. <https://doi.org/10.3389/fphys.2020.00768>.
- Islam, M.R., et al., 2013. Differential immune modulation by deoxynivalenol (vomitoxin) in mice. *Toxicol. Lett.* 221, 152–163. <https://doi.org/10.1016/j.toxlet.2013.05.656>.
- Ji, F., et al., 2014. Natural occurrence of deoxynivalenol and zearalenone in wheat from Jiangsu province, China. *Food Chem.* 157, 393–397. <https://doi.org/10.1016/j.foodchem.2014.02.058>.
- Kang, R., et al., 2019. Deoxynivalenol induced apoptosis and inflammation of IPEC-J2 cells by promoting ROS production. *Environ. Pollut.* 251, 689–698. <https://doi.org/10.1016/j.envpol.2019.05.026>.
- Khezri, A., et al., 2018. Mycotoxins induce developmental toxicity and behavioural aberrations in zebrafish larvae. *Environ. Pollut.* 242, 500–506. <https://doi.org/10.1016/j.envpol.2018.07.010>.
- Konig, J., et al., 2016. Human intestinal barrier function in health and disease. *Clin. Transl. Gastroenterol.* 7, e196. <https://doi.org/10.1038/ctg.2016.54>.
- Lassen, K.G., Xavier, R.J., 2018. Mechanisms and function of autophagy in intestinal disease. *Autophagy* 14, 216–220. <https://doi.org/10.1080/15548627.2017.1389358>.

- Li, M., et al., 2018a. Survey of deoxynivalenol contamination in agricultural products in the Chinese market using an ELISA Kit. *Toxins* 11. <https://doi.org/10.3390/toxins11010006>.
- Li, R., et al., 2018b. Short-term ingestion of deoxynivalenol in naturally contaminated feed alters piglet performance and gut hormone secretion. *Anim. Sci. J.* 89, 1134–1143. <https://doi.org/10.1111/asj.13034>.
- Li, B., et al., 2019. Inhibition of autophagy attenuated intestinal injury after intestinal I/R via mTOR signaling. *J. Surg. Res.* 243, 363–370. <https://doi.org/10.1016/j.jss.2019.05.038>.
- Liao, Y., et al., 2018. Deoxynivalenol, gut microbiota and immunotoxicity: a potential approach? *Food Chem. Toxicol.* 112, 342–354. <https://doi.org/10.1016/j.fct.2018.01.013>.
- Liu, D., et al., 2020a. Two-way immune effects of deoxynivalenol in weaned piglets and porcine alveolar macrophages: due mainly to its exposure dosage. *Chemosphere* 249, 126464. <https://doi.org/10.1016/j.chemosphere.2020.126464>.
- Liu, D., et al., 2020b. Low-level contamination of deoxynivalenol: a threat from environmental toxins to porcine epidemic diarrhea virus infection. *Environ. Int.* 143, 105949. <https://doi.org/10.1016/j.envint.2020.105949>.
- Lucke, A., et al., 2018. Dietary deoxynivalenol and oral lipopolysaccharide challenge differently affect intestinal innate immune response and barrier function in broiler chickens. *J. Anim. Sci.* 96, 5134–5143. <https://doi.org/10.1093/jas/sky379>.
- Macias-Ceja, D.C., et al., 2017. Stimulation of autophagy prevents intestinal mucosal inflammation and ameliorates murine colitis. *Br. J. Pharmacol.* 174, 2501–2511. <https://doi.org/10.1111/bph.13860>.
- Matsuzawa-Ishimoto, Y., et al., 2017. Autophagy protein ATG16L1 prevents necroptosis in the intestinal epithelium. *J. Exp. Med.* 214, 3687–3705. <https://doi.org/10.1084/jem.20170558>.
- Mir, H., et al., 2016. Occludin deficiency promotes ethanol-induced disruption of colonic epithelial junctions, gut barrier dysfunction and liver damage in mice. *Biochim. Biophys. Acta* 1860, 765–774. <https://doi.org/10.1016/j.bbagen.2015.12.013>.
- Mishra, S., et al., 2019. Global occurrence of deoxynivalenol in food commodities and exposure risk assessment in humans in the last decade: a survey. *Crit. Rev. Food Sci. Nutr.* 1–29. <https://doi.org/10.1080/10408398.2019.1571479>.
- Payros, D., et al., 2020. The food contaminant, deoxynivalenol, modulates the Thelper/Treg balance and increases inflammatory bowel diseases. *Arch. Toxicol.* 94, 3173–3184. <https://doi.org/10.1007/s00204-020-02817-z>.
- Peng, Z., et al., 2019. Heme oxygenase-1 attenuates low-dose of deoxynivalenol-induced liver inflammation potentially associating with microbiota. *Toxicol. Appl. Pharmacol.* 374, 20–31. <https://doi.org/10.1016/j.taap.2019.04.020>.
- Peyman, A., et al., 2014. Deoxynivalenol: a trigger for intestinal integrity breakdown. *Faseb Journal Official Publication of the Federation of American Societies for Experimental Biology* 28, 2414. <https://doi.org/10.1096/fj.13-238717>.
- Pierron, A., et al., 2018. Deepoxy-deoxynivalenol retains some immune-modulatory properties of the parent molecule deoxynivalenol in piglets. *Arch. Toxicol.* 92, 3381–3389. <https://doi.org/10.1007/s00204-018-2293-x>.
- Pinton, P., et al., 2008. Ingestion of deoxynivalenol (DON) contaminated feed alters the pig vaccinal immune responses. *Toxicol. Lett.* 177, 215–222. <https://doi.org/10.1016/j.toxlet.2008.01.015>.
- Piotrowska, M., et al., 2014. The effect of experimental fusarium mycotoxicosis on microbiota diversity in porcine ascending colon contents. *Toxins* 6, 2064–2081. <https://doi.org/10.3390/toxins6072064>.
- Pott, J., et al., 2018. Intestinal epithelial cell autophagy is required to protect against TNF-induced apoptosis during chronic colitis in mice. *Cell Host Microbe* 23, 191–202. <https://doi.org/10.1016/j.chom.2017.12.017> e194.
- Qian, G., et al., 2017. Ochratoxin A-induced autophagy in vitro and in vivo promotes porcine circovirus type 2 replication. *Cell Death Dis.* 8, e2909 <https://doi.org/10.1038/cddis.2017.303>.
- Reddy, K.E., et al., 2018. Effects of high levels of deoxynivalenol and zearalenone on growth performance, and hematological and immunological parameters in pigs. *Toxins* 10. <https://doi.org/10.3390/toxins10030114>.
- Romero, A., et al., 2016. Mycotoxins modify the barrier function of Caco-2 cells through differential gene expression of specific claudin isoforms: protective effect of illite mineral clay. *Toxicology* 353–354, 21–33. <https://doi.org/10.1016/j.tox.2016.05.003>.
- Sam, Q.H., et al., 2017. The fungal mycobiome and its interaction with gut bacteria in the host. *Int. J. Mol. Sci.* 18 <https://doi.org/10.3390/ijms18020330>.
- Scarpellini, E., et al., 2015. The human gut microbiota and virome: potential therapeutic implications. *Dig. Liver Dis. : official journal of the Italian Society of Gastroenterology and the Italian Association for the Study of the Liver* 47, 1007–1012. <https://doi.org/10.1016/j.dld.2015.07.008>.
- Shao, B.Z., et al., 2019. Targeting NLRP3 inflammasome in inflammatory bowel disease: putting out the fire of inflammation. *Inflammation* 42 (4), 1147–1159. <https://doi.org/10.1007/s10753-019-01008-y>.
- Su, J., et al., 2019. Long-time instead of short-time exposure in vitro and administration in vivo of ochratoxin A is consistent in immunosuppression. *J. Agric. Food Chem.* 67, 7485–7495. <https://doi.org/10.1021/acs.jafc.9b02595>.
- Sugiyama, K., et al., 2016. NF-kappaB activation via MyD88-dependent Toll-like receptor signaling is inhibited by trichothecene mycotoxin deoxynivalenol. *J. Toxicol. Sci.* 41, 273–279. <https://doi.org/10.2131/jts.41.273>.
- Wall-Martinez, H.A., et al., 2019. Frequency and levels of mycotoxins in beer from the Mexican market and exposure estimate for deoxynivalenol mycotoxins. *Mycotoxin Res.* <https://doi.org/10.1007/s12550-019-00347-x>.
- Wang, X., et al., 2019a. Eriodictyol ameliorates lipopolysaccharide-induced acute lung injury by suppressing the inflammatory COX-2/NLRP3/NF-kappaB pathway in mice. *J. Biochem. Mol. Toxicol.*, e22434 <https://doi.org/10.1002/jbt.22434>.
- Wang, X., et al., 2019b. Deoxynivalenol induces inflammatory injury in IPEC-J2 cells via NF-kappaB signaling pathway. *Toxins* 11, 733. <https://doi.org/10.3390/toxins11120733>.
- Wong, M., et al., 2017. Role of autophagy related protein ATG6/Beclin 1 in intestinal tight junction barrier. *Gastroenterology* 152, S119. <https://doi.org/10.1152/ajpcell.00246.2018>.
- Wu, J., et al., 2020a. β -Hydroxycholesterol-5-en-7-one from seahorse alleviates lipopolysaccharide-induced inflammatory responses by downregulating miR-98-5p. *Life Sci.* 118176. <https://doi.org/10.1016/j.lfs.2020.118176>.
- Wu, J., et al., 2020b. Betaine attenuates LPS-induced downregulation of Occludin and Claudin-1 and restores intestinal barrier function. *BMC Vet. Res.* 16, 75. <https://doi.org/10.1186/s12917-020-02298-3>.
- Xiao, L., et al., 2016. Long noncoding RNA SPRY4-IT1 regulates intestinal epithelial barrier function by modulating the expression levels of tight junction proteins. *Mol. Biol. Cell* 27, 617–626. <https://doi.org/10.1091/mbc.E15-10-0703>.
- Xie, M., et al., 2020. MiR-339 attenuates LPS-induced intestinal epithelial cells inflammatory responses and apoptosis by targeting TLR4. *Genes & genomics.* <https://doi.org/10.1007/s13258-020-00977-x>.
- Yamoto, M., et al., 2019. The role of autophagy in intestinal epithelial injury. *Pediatr. Surg. Int.* 35, 1389–1394. <https://doi.org/10.1007/s00383-019-04566-2>.
- Ying, C., et al., 2019. Nontoxic concentrations of OTA aggravate DON-induced intestinal barrier dysfunction in IPEC-J2 cells via activation of NF- κ B signaling pathway. *Toxicol. Lett.* 311, 114–124. <https://doi.org/10.1016/j.toxlet.2019.04.021>.
- Yu, M., et al., 2019. Deoxynivalenol induced mRNA expressions of inflammation and apoptosis in BeWo cells. *Wei sheng yan jiu = Journal of hygiene research* 48, 94–98. PMID: 31032775.
- Zeisel, M.B., et al., 2019. Tight junction proteins in gastrointestinal and liver disease. *Gut* 68, 547–561. <https://doi.org/10.1136/gutjnl-2018-316906>.
- Zhao, Y., et al., 2018. Deoxynivalenol in wheat from the Northwestern region in China. *Food Addit. Contam. Part B Surveill* 11, 281–285. <https://doi.org/10.1080/19393210.2018.1503340>.
- Zmora, N., et al., 2017. Inflammasomes and intestinal inflammation. *Mucosal Immunol.* 10, 865–883. <https://doi.org/10.1038/mi.2017.19>.